Available online at www.sciencedirect.com
SCIENCE DIRECT®
Pergamon
Cement and Concrete Research 34 (2004) 949–955
CEMENT AND CONCRETE RESEARCH

Zeolite formation in alkali-activated cementitious systems

Michael Grutzeck*, Stephen Kwan, Maria DiCola

104 Materials Research Laboratory, Materials Research Institute, The Pennsylvania State University, University Park, PA 16802, USA

Received 13 June 2002; accepted 3 November 2003

Abstract

Autoclaved aerated concrete (AAC) is a unique building material. Because of its cellular nature, it is lightweight, self-insulating, sound- and fireproof, as well as insect and mold resistant. Furthermore, AAC is free of VOCs and various fibers associated with wood and glass wool construction. In an attempt to toughen AAC and make it less prone to on-site damage, a conventional fly-ash-based AAC formulation is being supplemented with sodium hydroxide (NaOH). The introduction of sufficient alkali promotes the growth of crystalline zeolites in the tobermorite matrix during autoclave curing. It is postulated that in situ grown zeolites will serve the same purpose as added fibers. Inasmuch as fly-ash-based AAC reactions often do not go to completion, a phase study of the development of tobermorite and zeolites from a gel-like slurry made from reagent grade chemicals was undertaken. Mixtures were studied as a function of time and temperature. Phase development depends on bulk composition and curing conditions. Longer curing at higher temperatures causes the Na-P1 that forms initially to change to analcime. Whereas Na-P1 is bladelike in habit and is seen to intermingle with the slightly larger blades of tobermorite, the Na-P1 gradually undergoes a phase change to analcime that forms very large cubes. This change has the potential to disrupt the AAC matrix.

Keywords: Alkali-activated cement; Zeolite; Hydration; Characterization; SEM; X-ray diffraction

1. Introduction

Autoclaved aerated concrete (AAC) has unique characteristics. It is a lightweight building material that consists of a mixture of calcium silicate hydrate (C-S-H), tobermorite and gas-filled voids. AAC is normally manufactured from a mixture of finely ground silica sand or fly ash, Portland cement, lime and water. Its cellular character is obtained by adding aluminum powder to the mixture at the very last minute, pouring the slurried mixture into a mold, and then allowing it to rise much like a cake rises in the oven. After the ''cake'' gains enough ''green strength'' to allow it to be demolded, the cake is cut into desired shapes using gangs of wire saws. The cut block or panel is then autoclaved at 180 °C for 10 to 16 h depending on whether the AAC contains wire-cage reinforcement. In addition to its light weight, AAC is also thermally insulating, sound- and fireproof, and insect and mold resistant. In the long term, the additional cost of a slightly more expensive AAC vis-à-vis wood frame/glass-wool-insulated house is actually a good investment because AAC is virtually maintenance free. Longevity is a given fact with an AAC house; it will essentially last forever [1].

AAC block and panel are established building materials in most countries that have little or no timber of their own. It was used to rebuild much of Europe after World War II and currently more than 50% of the housing in Japan is constructed using AAC. Unfortunately for the manufacturers of AAC, North America is blessed with a nearly endless supply of timber and governments that tend to subsidize the industry by allowing logging on public lands. This combination provides an abundant supply of low-cost lumber, which in turn makes wood-based construction affordable. Given the status quo, there is little reason to change. For example, two German companies (Ytong and Hebel) spent countless millions of dollars and about 10 years each trying to make inroads into the American market. Both failed. Perhaps expectation exceeded demand. Hebel was purchased by J.A. Jones and other parties in 1999 and continued to operate but under the name of Matrix. In 2001, Matrix was purchased by Babb International, who is currently operating the plant and producing both silica sand AAC and a blended silica sand/fly ash AAC. The Ytong plant remained empty for several years until it was purchased by Aercon Industries (a

* Corresponding author. Tel.: +1-814-863-2779; fax: +1-814-863-7040.
E-mail address: gur@psu.edu (M. Grutzeck).

0008-8846/$ – see front matter © 2004 Elsevier Ltd. All rights reserved.
doi:10.1016/j.cemconres.2003.11.003

group of investors based in Indianapolis) in September 2002. Aercon Industries produces silica sand AAC. ACCO Aerated Concrete Systems was built by Florida Crushed Stone and continues to produce silica sand AAC. E-Crete based in Arizona has recently started to manufacture and market AAC made from mine tailings. Much like fly ash, mine tailings are silica rich and can be used to make AAC.

AAC is slowly gaining acceptance in the United States. It is being used in increasing amounts for the construction of industrial, office and public buildings where its acceptance has been very good. It has characteristics that make its use perfect for schools, multiplexes and multitenant buildings where sound transmission is a problem. Also it is perfect for those in need of allergy-free housing. In order to make the best AAC possible, research was initiated to address its inherent brittleness. AAC tends to suffer edge damage and/or break if it is bumped or dropped. This characteristic often gives the material a bad reputation when used for the first time by individuals used to handling cement block. The research described below is part of an ongoing effort to toughen fly-ash-based AAC with in situ growth of zeolites in a C-S-H (tobermorite) matrix. Zeolites are members of a mineral class called tectosilicates, a structure type typified by quartz. The term tectosilicate brings to mind an image of multiple silicate tetrahedra, each bonded to four other silicate tetrahedra. Zeolites differ from quartz in two ways. Zeolites have open structures built around large solvated cations such as sodium or potassium. The silicate network forms around the ions resulting in low-density materials (~ 2 g/cm^3) containing cavities and channels. The large cations have positive charges. The structure is charge compensated by the substitution of an aluminum ion for a silicate ion in selected tetrahedra. For example, analcime ($NaAlSi_2O_6 \cdot H_2O$) is a common zeolite. The ion pair AlSi has replaced one Si ion [2].

2. Experimental method

Zeolites can be synthesized by mixing fly ash with highly alkaline sodium hydroxide solution [3–18]. In order to evaluate the effects of adding sodium hydroxide to fly-ash-based AAC, a series of experiments were undertaken to determine the phase chemistry of the system. When making AAC from fly ash, reactions often do not go to completion. Equilibrium is not attained and thus it is somewhat difficult to determine the phase chemistry of the reaction [19]. Most samples contain small amounts of residual fly ash and cement clinker phases. To eliminate this problem, a solution representing the chemical equivalent of a 50:50 blend of zeolite Na-P1 ($3Na_2O \cdot 3Al_2O_3 \cdot 10SiO_2 \cdot 12H_2O$) and tobermorite ($0.8\ CaO \cdot SiO_2 \cdot xH_2O$) was prepared from Ludox (Dupont/W.R. Grace), purified sodium aluminate (Fisher Scientific), and high-fired calcium oxide (Mississippi Lime).

The bulk composition (by weight) calculated for the above mix was 21.5% CaO, 8.5% Na_2O, 14.0% Al_2O_3 and 56.0% SiO_2. The needed Ludox (903.2 g of 62 wt.% SiO_2), sodium aluminate (300 g $Na_2Al_2O_4 \cdot 3H_2O$) and calcium oxide (215 g CaO) were each mixed with enough DI water to make ~ 500 ml of suspension/solution. This was done to allow the lime to slake and to facilitate final mixing. The three suspensions/solutions were then poured simultaneously into a stainless steel beaker (Vollrath) with continuous stirring (Stir-pak/Cole-Parmer Instrument). The mixture self-heated to approximately 38 °C. Stirring continued for about 24 h to permit nucleation and gelling. The mixture was then permitted to settle for another 24 h. The pH of the liquid at the top of the sample was ~ 13. The mixture was then placed in a 110 °C oven overnight to dry.

By morning, a moist, white gel, approximately 2 in. thick, had formed on top of the sample. Before remixing the gel and remaining liquid, a small amount of the gel was taken from the upper surface, dried at 110 °C and analyzed using a Sintag X-ray diffractometer (Sintag) equipped with Cu Kα radiation and operating at a 2° per minute scan speed. Three 5-g samples of the moist gel were also taken and placed into Teflon-lined Parr bombs (Parr Instrument) with an additional 10 g of deionized water. The Parr bombs were placed into ovens (Blue M and Yamoto) at 110, 150 and 200 °C and cured under saturated steam pressure for 2 days. The Parr bombs were removed, cooled and weighed to determine if the vessels had leaked (they did not). The Parr bomb samples were dried at 110 °C and X-rayed.

When the remaining bulk of the gel and liquid were remixed, a slurry formed that was white in color and had a pH of 12. The water content of the slurry was determined by drying a small amount of the gel for approximately 72 h at 110 °C. The slurry contained about two parts water to one part solid, approximately the same ratio as the initial gel plus water experiments. To check similarity of outcome, a sample of the slurry was cured at 200 °C for 90 h; phase development in both samples was identical. At this point it was decided to use the slurried gel as the starting material for the remaining experiments. Typically, samples of the slurried gel were placed into Parr bombs without adding extra water. The Parr bombs were heated to 115, 150 and 200 °C for 0.5, 1, 3 and 7 days wherein the samples were exposed to saturated steam pressure. Afterwards, the Parr bombs were cooled and weighed to determine water loss, if any, the sample removed and dried at 110 °C before X-ray diffraction analysis. Finally, additional runs in Parr bombs were made at 150, 180 and 200 °C and examined with the scanning electron microscope (Hitachi S2000). As shown below, there was a definite relationship between phase development, time and temperature of curing.

3. Results

Fig. 1 consists of a compilation of X-ray diffraction patterns of the initial 5-g gel samples mixed with an

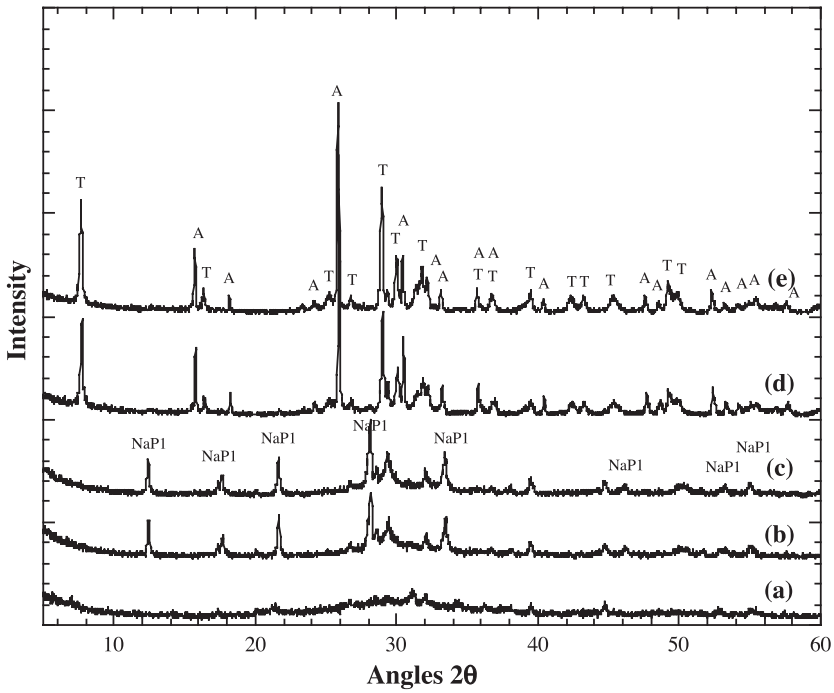

Fig. 1. X-ray diffraction patterns for samples cured for 2 days. (a) Represents the untreated gel starting material. (b) Represents the gel after heating at 110 °C; it contains Na-P1 and C-S-H (broad amorphous hump centered at ~ 30° 2θ). (c) Represents the gel cured at 150 °C. Its pattern is the same as its predecessor. (d) Represents the 200 °C treated sample. It contains tobermorite, a crystalline C-S-H (T), and a trace of analcime (A). (e) Pattern for the remixed gel slurry cured at 200 °C. (d) and (e) are essentially identical.

additional 10 g of water (b–d) and a slurry sample (e) that were each cured at three temperatures for 2 days. View (a) represents the gel itself before curing. It is devoid of crystalline material. It does, however, contain C-S-H as indicated by the presence of an amorphous hump centered at ~ 30° 2θ. Results of the curing trials made in Parr

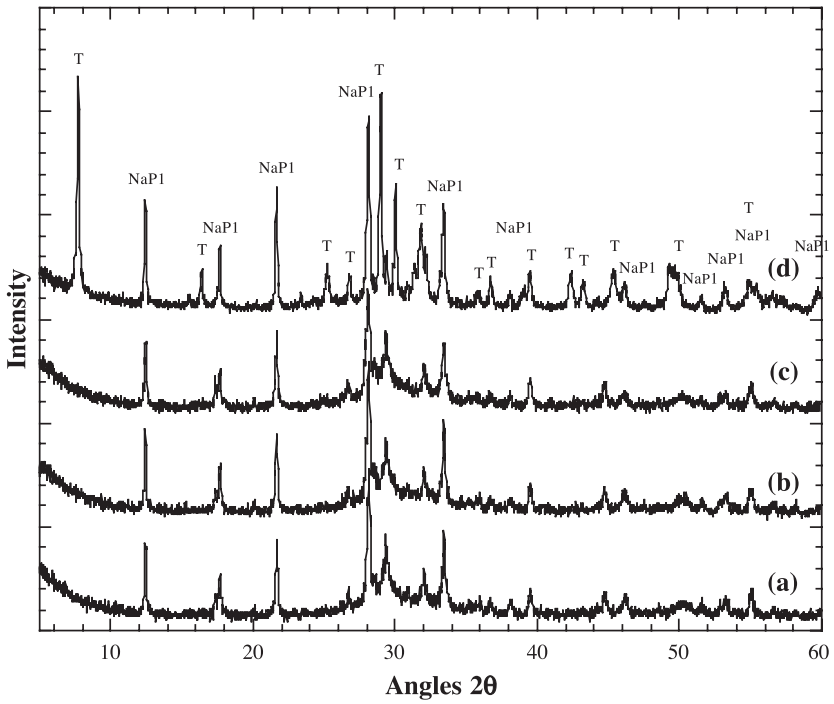

Fig. 2. X-ray diffraction patterns for gel samples cured at 115 °C for (a) 0.5, (b) 1, (c) 3 and (d) 7 days. The 0.5- to 3-day samples (a–c) contain a mixture of Na-P1 and C-S-H (broad amorphous hump centered at ~ 30° 2θ). The 7-day sample (d) contains tobermorite (T) and Na-P1.

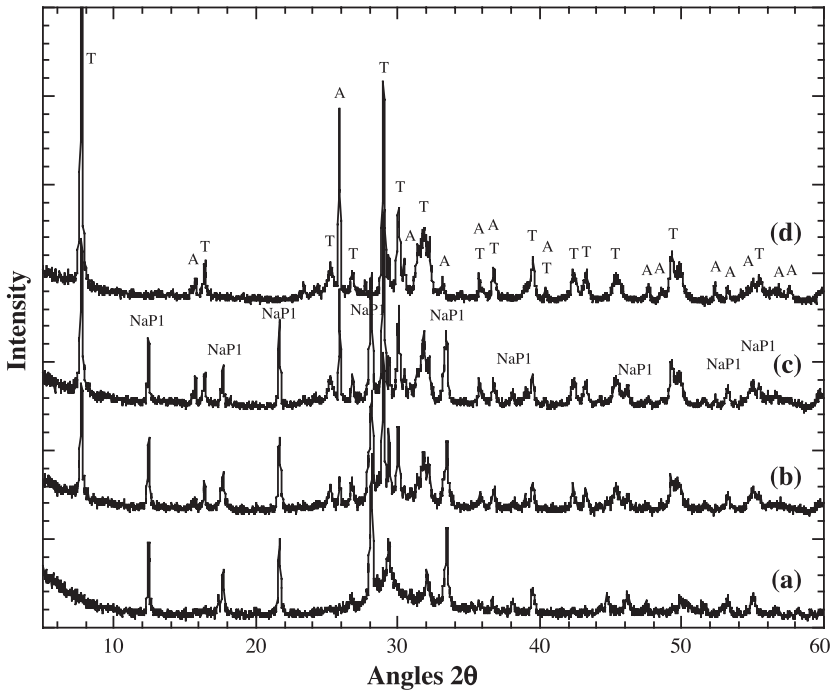

Fig. 3. X-ray diffraction patterns for gel samples cured at 150 °C for (a) 0.5, (b) 1, (c) 3 and (d) 7 days. The 0.5-day sample (a) contains a mixture of Na-P1 and C-S-H (broad amorphous hump centered at ~ 30° 2θ). The 1- to 3-day samples (b–c) contain tobermorite (T), Na-P1 and a trace of analcime (A). The 7-day sample (d) contains tobermorite (T) and analcime (A).

bombs at 110, 150 and 200 °C are given in views (b–d), respectively. View (e) represents a slurried gel sample that was cured without additional water at 200 °C. Both samples (d and e) have identical phase development, confirming the similarity of results obtained using the two types of gel samples.

The samples heated at 110 (b) and 150 °C (c) contain Na-P1and a small amount of X-ray amorphous C-S-H. The

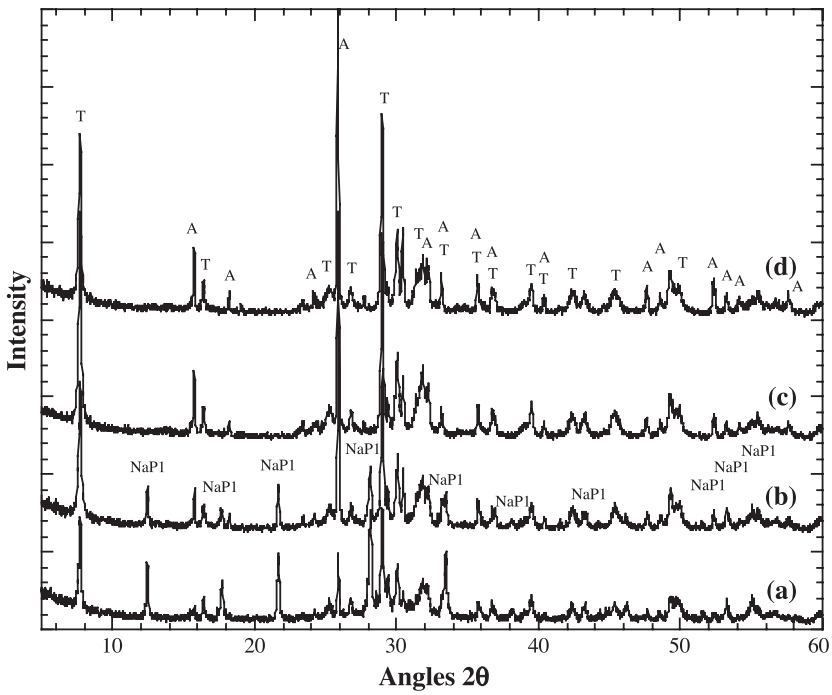

Fig. 4. X-ray diffraction patterns for gel samples cured at 200 °C for 0.5, 1, 3 and 7 days. The 0.5 day sample (a) contains a mixture of Na-P1 and tobermorite (T) and a trace of analcime (A). The 1-day sample (b) contains tobermorite (T), Na-P1 and analcime (A). The 3- and 7-day samples (c–d) contain tobermorite (T) and analcime (A).

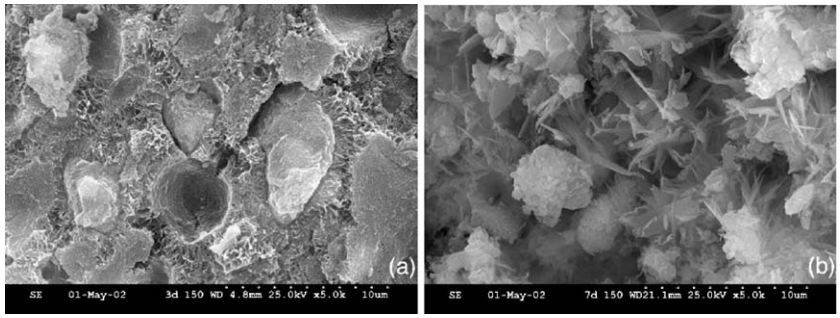

Fig. 5. SEM images (5000 ×) of samples cured at 150 °C for (a) 3 and (b) 7 days. Both Na-P1 and zeolite A are seen to coexist with C-S-H/tobermorite matrix.

sample cured at 200 °C (d) contains tobermorite and analcime rather than Na-P1. Kinetics may play a role here; Na-P1 is probably an intermediate phase that forms prior to analcime. At least this is the case in nature. Because of these preliminary experiments, remixed slurry was used as starting material for the remaining work. Results for a second set of tests made with the remixed slurry after curing as a function of time and temperature are given in Figs. 2–4. Fig. 2 represents data for samples cured at 115 °C for 0.5, 1, 3 and 7 days in Teflon lined Parr bombs. Interestingly, all samples contained Na-P1. Na-P1 is stable for longer periods at this temperature, but it took 7 days for tobermorite to crystallize. Fig. 3 represents data for runs made at 150 °C. In this instance tobermorite begins to crystallize at 1 day. Na-P1 is stable for a day or so, after which it begins to coexist with a trace of analcime. By 7 days, the Na-P1 has decomposed and tobermorite now coexists with analcime. Fig. 4 represents the data for the runs performed at 200 °C. In this instance, temperature has accelerated the kinetic process for both the crystallization of C-S-H to tobermorite and the conversion of Na-P1 to analcime. It is clear that time and temperature play an important role in governing the phase development of a given sample. The consequences of the phase change phenomena are explored in the next section.

A series of scanning electron microscope (SEM) images of three additional samples cured as above but at 150, 180 and 200 °C as a function of time were taken to explore the consequences of phase change on microstructure. The 150 °C 3-day sample shown in Fig. 5 was cured for 3 and 7 days, respectively. The 3-day sample (a) has developed a reticulated microstructure around residual clumps of the gel starting material. Some casts remain where the particles were plucked out during sample preparation. The reticulated material is a combination of tobermorite and C-S-H and, presumably, the larger clumps contain the Na-P1 and smaller amounts of zeolite A crystals identified in the X-ray diffraction patterns. The 7-day sample contains crystalline tobermorite, zeolite A and minor amounts of Na-P1. Note that the microstructure is very different. Instead of having a continuous matrix as in the 3-day sample, the

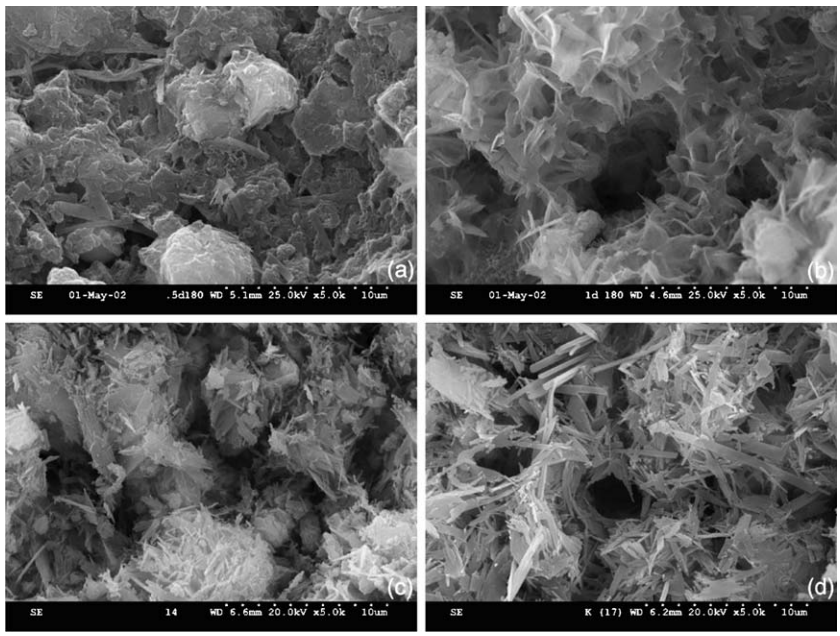

Fig. 6. SEM images (5000 ×) of samples cured at 180 °C for (a) 0.5, (b) 1, (c) 3 and (d) 7 days. Na-P1 forms first (a), it is joined by tobermorite (b), they are joined by analcime (c), and finally, the mix converts to tobermorite and analcime (d).

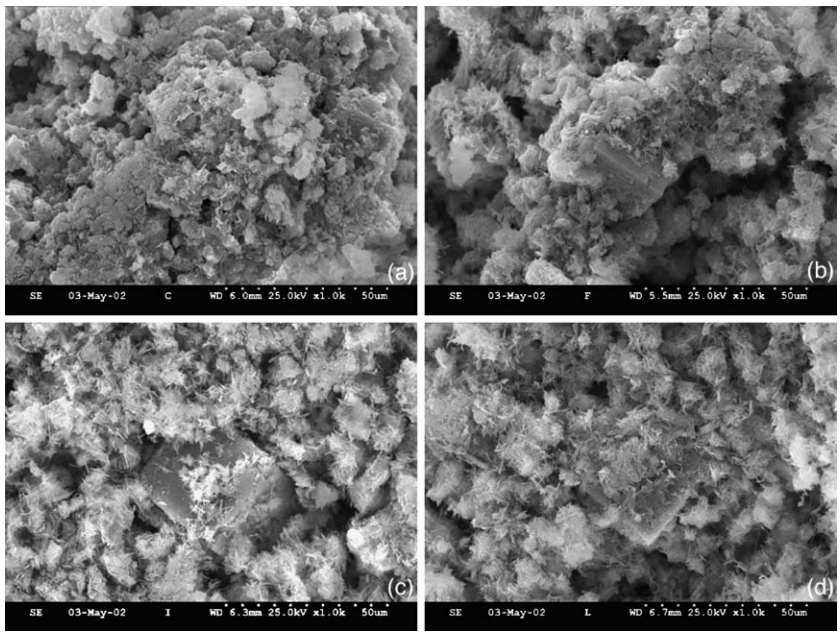

Fig. 7. SEM images (1000 ×) of samples cured at 200 °C for (a) 0.5, (b) 1, (c) 3 and (d) 7 days. (a) Contains tobermorite, Na-P1 and a trace of analcime cubes; (b) contains tobermorite, analcime and a lesser amount of Na-P1; (c) contains only tobermorite and analcime; and (d) contains mostly tobermorite and possibly resorbing analcime.

further crystallization of tobermorite has created a more porous matrix consisting of intergrown A, Na-P1 and tobermorite crystals. Fig. 6 represents data for samples cured at 180 °C. The 12-h sample contains Na-P1 and C-S-H. The bladelike character of the Na-P1 is quite evident. By 1 day, the sample has developed crystalline tobermorite. The resulting microstructure is highly porous, consisting of interlocking Na-P1 and tobermorite crystals. By 3 days, a trace of analcime appears. By 7 days, the sample consists of a mixture of tobermorite and analcime. The Na-P1 has dissolved and converted to analcime, which is in keeping with similar observed behavior for natural zeolites. Fig. 7 represents gel samples cured at 200 °C. The 12-h sample (a) contains crystalline tobermorite, Na-P1 and a trace of analcime (cubes). The sample's microstructure is very bladelike in appearance. The 1-day sample (b) consists predominantly of tobermorite, increased amount of analcime and a lesser amount of Na-P1. The latter is transforming into analcime. Because analcime forms large cubic crystals, the effect on the microstructure is striking. A cube edge can be seen at the center of (b). By 3 days (c) the sample consists of tobermorite and minor amounts of analcime; Na-P1 has been reabsorbed. The tobermorite is beginning to take on a more characteristic shape. At 7 days, tobermorite dominates the sample. It appears some of the analcime cubes are being reabsorbed as well.

4. Conclusions

Time and temperature dictate the nature of the final product. By extrapolating these data using phase pure material to fly-ash-based AAC, the data suggest that the autoclave process should be carried out at 180 or 200 °C for a maximum of 12–24 h. At this processing condition, the zeolite Na-P1 forms first followed closely by the crystallization of tobermorite. Na-P1 has a bladelike structure similar to tobermorite that forms at slightly longer times. The intergrowth of tobermorite and analcime could provide the toughening necessary to make AAC slightly more robust. It is also suggested that the formation of large analcime crystals have the potential to disrupt the integrity of a solid AAC sample and should be avoided. In an earlier paper, Grutzeck et al. [19] demonstrated that precuring temperature affected the strength of the final sample. A conventional fly-ash-based AAC that was precured at 90 °C rather than at 38 °C developed twice the strength of the 38 °C sample once they were autoclaved at 180 °C. Conversely, it was shown that an alkali-activated AAC similar in nature to the samples described in this paper benefited most by a precure at 38 °C. Precuring at 90 °C caused the sample to have half of the strength of the 38 °C sample once both were autoclaved. It is suggested that precuring the conventional material causes the sample to harden in two dramatically different ways. The 38 °C sample develops a lime-rich C-S-H having a Ca/Si molar ratio in excess of 1.0. The mixture is most likely dominated by sorosilicate C-S-H consisting of Si_2O_7 anions [20–22]. Upon autoclaving, these silicate anions must rearrange themselves to form dreierketten during the crystallization of tobermorite. The sample cured at 90 °C tends to form lime-poor C-S-H directly (Ca/Si < 1.1), which makes it easier to crystallize into tobermorite on autoclaving. The C-S-H contains dreierketten chains from the very beginning [20–22]. The alkali-

containing samples are thought to be affected in an opposite fashion. The 38 °C precured sample tends to form a larger quantity of zeolite precursor gel that crystallizes to a zeolite on heating to 180 °C. The gel has an abundance of short range order precursor crystallites that can move around and crystallize when autoclaved. The stable phase forms initially and continues to grow. On the other hand, the 90 °C curing causes zeolites to form at 90 °C that then must undergo transformation to another phase upon autoclaving at 180 °C, which disrupts the matrix. The data presented in this paper would seem to substantiate the proposed mechanisms, however, follow-up experiments are planned to prove both of the initially mentioned conclusions.

Acknowledgements

This material is based on work supported by the National Science Foundation under Grant No. 9988534.

References

[1] C.A. Fudge, A.R. Riza, The practical use of AAC masonry to meet the performance requirements of buildings in Europe, in: F.H. Wittmann (Ed.), Advances in Autoclaved Aerated Concrete, A.A. Balkema, Rotterdam, 1992, pp. 231–236.
[2] D.W. Breck, Zeolitic Molecular Sieves, Wiley-Interscience, New York, 1974.
[3] T. Henmi, Synthesis of hydroxy-sodalite (“zeolite”) from waste coal ash, Soil Sci. Plant Nutr. 33 (1987) 517–521.
[4] F. Mondragon, F. Rincon, L. Sierra, J. Escobar, J. Ramirez, J. Fernandez, New perspectives for coal ash utilization: synthesis of zeolitic materials, Fuel 69 (1990) 263–266.
[5] J. LaRosa, S. Kwan, M.W. Grutzeck, Self-generating zeolite cement composites, in: F.P. Glasser, G.J. McCarthy, J.F. Young, T.O. Mason, P.L. Pratt (Eds.), Advanced Cementitious Systems: Mechanisms and Properties, Materials Research Society Symposium Proceedings, vol. 245, Materials Research Society, Pittsburgh, PA, 1991, pp. 211–216.
[6] J. LaRosa, S. Kwan, M.W. Grutzeck, Zeolite formation in class F fly ash blended cement pastes, J. Am. Ceram. Soc. 75 (1992) 1574–1580.
[7] N. Shigemoto, K. Shirakami, S. Hirano, H. Hayashi, Preparation and characterization of zeolites from coal ash, Nippon Kagaku Kaishi 1992 (1992) 484–492.
[8] N. Shigemoto, H. Hayashi, K. Miyaura, Selective formation of Na-X zeolite from coal fly ash by fusion with sodium hydroxide prior to hydrothermal reaction, J. Mater. Sci. 28 (1993) 4781–4786.
[9] N. Shigemoto, S. Sugiyama, H. Hayashi, K. Miyaura, Characteristics of NaX, Na-A, and coal fly ash zeolites and their amorphous precursors by IR, MAS NMR and XPS, J. Mater. Sci. 30 (1995) 5777–5783.
[10] H.-L. Chang, W.-H. Shih, Conversion of fly ashes to zeolites for waste treatment, in: V. Jain, R. Palmer (Eds.), Environmental Issues and Waste Management Technologies, Ceramic Transactions vol. 61, American Ceramic Society, Westerville, OH, 1995, pp. 81–88.
[11] C.-F. Lin, H.-C. Hsi, Resource recovery of waste fly ash: synthesis of zeolite-like materials, Environ. Sci. Technol. 29 (1995) 1109–1117.
[12] M. Park, J. Choi, Synthesis of phillipsite from fly ash, Clay Sci. 9 (1995) 219–229.
[13] X. Querol, A. Alastuey, J.L. Fernandez-Turiel, A. Loez-Soler, Synthesis of zeolites by alkaline activation of ferro-aluminous fly ash, Fuel 74 (1995) 1226–1231.
[14] X. Querol, A. Alastuey, A. Lopez-Soler, F. Plana, J.M. Andres, R. Juan, P. Ferrer, C.R. Ruiz, A fast method for recycling fly ash: microwave-assisted zeolite synthesis, Environ. Sci. Technol. 31 (1997) 2527–2533.
[15] W.-H. Shih, H.-L. Chang, Z. Shen, Conversion of class-F fly ash into zeolites, in: S. Komarneni, D.M. Smith, J.S. Beck (Eds.), Advances in Porous Materials, Materials Research Society Symposium Proceedings, vol. 371, Materials Research Society, Pittsburgh, PA, 1995, pp. 39–44.
[16] A. Singer, V. Berkgatit, Cation exchange properties of hydrothermally treated coal fly ash, Environ. Sci. Technol. 29 (1995) 748–753.
[17] C. Amrhein, G.H. Haghnia, T.S. Kim, P.A. Mosher, R.C. Gagaiena, T. Amanios, L. de La Torre, Synthesis and properties of zeolites from coal fly ash, Environ. Sci. Technol. 30 (1996) 735.
[18] Y. Suyama, K. Katayama, M. Meguro, NH^{4+}-adsorption characteristics of zeolites synthesized from fly ash, Nippon Kagaku Kaishi 2 (1996) 136–140.
[19] M.W. Grutzeck, S. Kwan, M. DiCola, Alkali activated autoclaved aerated concrete: effect of precuring temperature, in: G. Grieve, G. Owens (Eds.), Proceedings 11th International Congress on the Chemistry of Cement (ICCC), Cement’s Contribution to the Development in the 21st Century, Cement and Concrete Institute, Durban, South Africa, 2003, pp. 1248–1259.
[20] M.W. Grutzeck, J. LaRosa-Thompson, S. Kwan, Characteristics of C-S-H gels, in: H. Justnes (Ed.), Proceedings 10th International Congress on the Chemistry of Cement, Gothenburg, Sweden, Amarkai AB and Congrex Göteborg AB, Göteborg, Sweden, 1997. 2ii067.
[21] M.W. Grutzeck, A new hydration model for calcium silicate hydrate (C-S-H), Mater. Res. Innov. 3 (1999) 160–170.
[22] M.W. Grutzeck, S. Kwan, J. LaRosa Thompson, A.A. Benesi, A sorosilicate model for calcium silicate hydrate, J. Mater. Sci. Lett. 18 (1999) 217–220.